Eur J Plant Pathol (2018) 151:57–72
DOI 10.1007/s10658-017-1349-8

Bimetallic blends and chitosan nanocomposites: novel antifungal agents against cotton seedling damping-off

Kamel A. Abd-Elsalam · Alexander Yu. Vasil'kov · Ernest E. Said-Galiev · Margarita S. Rubina · Alexei R. Khokhlov · Alexander V. Naumkin · Eleonora V. Shtykova · Mousa A. Alghuthaymi

Accepted: 21 September 2017 / Published online: 2 October 2017

Abstract Phytopathological studies of chitosan nanocomposites are mainly focused on in vitro efficiency, so it is essential to perform a complementary greenhouse assay to find eco-friendly alternatives for plant disease management. In the present study, Cu-chitosan and Zn-chitosan nanocomposites were prepared by reduction of metal precursors in the presence of chitosan in sc CO_2 medium and deposition of organosol on chitosan, respectively. Physicochemical properties of the nanocomposites were characterized by X-ray fluorescence analysis (XRF), Small angles X-ray Scattering (SAXS), X-ray Photoelectron spectroscopy (XPS), and Transmission electron microscopy (TEM). The bimetallic blends (BBs) based on nanoscale $Cu(OH)_2$ were obtained through simple precipitation and grinding methods. In vitro and in vivo studies of the antifungal activity of Cu-chitosan, Zn-chitosan and BBs at concentrations of 30, 60, and 100 μg ml^{-1} were conducted against two anastomosis groups of *Rhizoctonia solani* for control of cotton seedling damping-off. Effect of metal-chitosan nanocomposites at 100 μg ml^{-1} combined with Cu-tolerant *Trichoderma longibrachiatum* strains was also evaluated for control of cotton seedling damping-off under greenhouse conditions. The BBs and Cu-chitosan nanocomposite showed the highest antifungal efficacy against both anastomosis groups of *R. solani* in vitro. These results indicated that BBs, Cu-chitosan nanocomposite, and BBs combined with *Trichoderma* may suppress cotton seedling disease caused by *R. solani* in vivo. The evaluation of *R. solani* in a greenhouse with a *Trichoderma* strain showed synergistic inhibitory effect with BBs. Light micrographs of mycelia treated with BBs showed the disruption of the hyphal structures. The interaction of the nanocomposites with DNA isolated from the exposed fungal cells, by means of bonding and/or degradation, was also investigated. DNA interaction in terms of binding and degradation for treated DNA with BBs and chitosan nanocomposites was demonstrated. The results showed the absence of DNA amplification by a microsatellite primed PCR.

Keywords Biocompatibility · *Rhizoctonia solani* · *Trichoderma longibrachiatum* · Bimetallic nanocomposite · Cu-chitosan · Zn-chitosan · Nanoscale $Cu(OH)_2$

K. A. Abd-Elsalam (✉)
Plant Pathology Research Institute, Agricultural Research Center (ARC), 9 Gamaa St, Giza 12619, Egypt
e-mail: kamelabdelsalam@gmail.com

K. A. Abd-Elsalam
Unit of Excellence in Nano-Molecular Plant Pathology Research Center – Plant Pathology Research Institute, Giza, Egypt

A. Y. Vasil'kov · E. E. Said-Galiev · M. S. Rubina · A. R. Khokhlov · A. V. Naumkin
A.N. Nesmeyanov Institute of Organoelement Compounds of Russian Academy of Sciences (INEOS RAS), Moscow, Russia

E. V. Shtykova
A.V. Shubnikov Institute of Crystallography of Russian Academy of Sciences (IC RAS), Moscow, Russia

M. A. Alghuthaymi
Biology Department, Science and Humanities College, Shaqra University, Alquwayiyah, Saudi Arabia

Introduction

Rhizoctonia solani (Kühn) is an important necrotrophic fungal pathogen, with a broad host range and many susceptible crops lack cultivar resistance to this fungal pathogen (Nikraftar et al. 2013). Managing *R. solani* is difficult because of the formation of sclerotia which can survive in harsh environmental conditions. Therefore the development of new eco-friendly nanocides has been considered important to maintain sustainable agriculture (Abd-Elsalam and Khokhlov 2015; Abd-Elsalam and Alghuthaymi 2015; Soltani-Nejad et al. 2016).

The high costs and other disadvantages of chemical controls of fungal pathogens have encouraged a search for alternative methods to control plant disease (Jans et al. 2014; Yoon et al. 2013). Previous studies have evaluated the combined antimicrobial effect of inorganic nanoparticles with bioorganic pesticides for controlling plant diseases in the greenhouse and open field (Joselito and Soytong 2014; Xue et al. 2014). The use of a combination of active ingredients may increase antifungal activity by synergistic interaction, which may reduce fungicide dose and consequently avoid development of fungal pathogen resistance (Soytong et al. 2013).

Biopolymer derivatives such as chitosan are recommended as biofungicides for control of plant diseases (Muzzarelli et al. 2001; Saharan et al. 2013). Chitosan-induced inhibition has been previously studied at different fungal developmental stages such as mycelial growth, sporulation, spore viability and germination, and the production of fungal virulence factors (Xu et al. 2007a). Chitosan can also be used as a seed coating agent for increasing resistance of host plants (Reddy et al. 1999). There are many methods for introducing metal nanoparticles in polymers. The first promising method for obtaining metal-polymer nanocomposites (NCs) by using supercritical media or fluids. Supercritical carbon dioxide (sc CO_2) is the best known medium for these purposes (Said-Galiev et al. 2011). Another efficient method to obtain metal-polymer NCs with biological activity is metal-vapor synthesis (MVS) (Nikitin et al. 2011). The MVS method involves preparing dispersion of nanoparticles in diverse solvents like acetone, i-PrOH, diglym, toluene and others (Stoeva et al. 2007). The prepared nanoparticles colloidal solution called organosol is used for modification of different types of materials (Rubina et al. 2016). Bimetallic nanocomposites can replace chemical pesticides in controlling and inhibiting sheath blight in rice caused by *R. solani* (Soltani-Nejad et al. 2016). Cu–chitosan NCs can be used as antifungal agents against early blight and Fusarium wilt of tomato (Saharan et al. 2015). The combined copper (II) chitosan colloids are being used as a new generation of copper-based bio-pesticides (Brunel et al. 2013). Examples of metal-polymer composites designed to have antimicrobial activities, with a special focus on copper and silver metal nanoparticles and their mechanisms, have been previously reviewed by Palza (2015). Chitosan-metal NCs can be effectively used against various plant pathogenic fungi to protect a range of crop plants and their products (Kaur et al. 2015). In the current work, the novel chitosan NCs and BBs based on nanoscale $Cu(OH)_2$ were prepared. The antifungal activities of the prepared nanomaterials were tested in different concentrations against two *R. solani* anastomosis groups through in vitro mycelial growth and sclerotia formation assays. Greenhouse experiments were performed to evaluate the influence of the synthesized materials combined with a Cu-tolerant *Trichoderma* strain for control of cotton damping-off disease caused by *R. solani.* The effects of BBs and the nanocomposites on genotoxicity were also evaluated. To the best of our knowledge, this is the first report demonstrating use of BBs and chitosan NCs as antifungal agents against cotton seedling damping-off.

Material and methods

Reagents and chemicals

Special purity grade toluene (99.5%) was used as the solvent for MVS. Prior to synthesis, toluene was dried over Na and then degassed under vacuum of 10^{-1} Pa by using freeze-thaw cycles. Zn granules (purity ≥99.8%, "Sigma-Aldrich, USA") were evaporated by resistively heating a tantalum boat (90 × 5 mm) at a residual pressure of 10^{-5} Torr. Low molecular weight chitosan (≤200 mPa*s, DD > 85%, "Wirud, Germany") was used as a matrice. The organometalic complex copper(II) 1,1,1,5,5,5-hexafluoroacetylacetonate hydrate $Cu(hfacac)_2 \cdot xH_2O$, (x < 1), (a greenish blue substance), mp 403–407 K, solubility in sc CO_2 at 313 K and 13.8 MPa is 0.13 mol/L (0.064 g/cm^3) (Fedotov et al. 1997) was used as a metal precursor for synthesis in sc CO_2 medium. The complex was purchased from

"Sigma-Aldrich, USA" and used without additional purification. Carbon dioxide and hydrogen with high purity were purchased from Moscow Plant of pure gases "Linde gas". For preparation of bimetallic blends, $CuSO_4 \cdot 5H_2O$, NaOH and K_3PO_4 were analytical grade.

Preparation of Zn-chitosan nanocomposite

The nanocomposite was made by impregnation of low molecular weight chitosan with metal organosol. The organosol was prepared with metal-vapor synthesis according to the procedure described previously (Vasil'kov et al. 2010). The experimental setup of MVS has been described before (Vasil'kov et al. 1995). In a typical experiment, 0.5 g of Zn granules, 120 ml of toluene and 4 g of chitosan were used. Molar ratio of metal: solvent was 1:150. During the first stage, metal and vapor of solvent were condensed on liquid nitrogen-cooled walls of a 5 L reactor. Next, the deposit was melted, and the resulting metal organosol (Zn-toluene) was infiltrated into chitosan powder in an evacuated Schlenk vessel. The excess organosol was removed, and the support was dried under vacuum of 1 Pa at 363 K during 1 h. During the final stage the powder of Zn-chitosan NC was prepared. All manipulations were performed in pure Ar atmosphere. Before the modification by metal nanoparticles, chitosan was degassed for 4 h under vacuum of 10^{-1} Pa at 313 K.

Preparation of Cu-chitosan nanocomposite

The experimental setup of fluid technology has been described before (Said-Galiev et al. 2011). The synthetic fluid technology for production of metal NC included 4 stages: 1- chitosan drying under vacuum at the temperature of 373 K; 2 - impregnation of chitosan with $Cu(hfacac)_2 \times H_2O$ in sc CO_2 solution (333 K, 7.5 MPa, 10 h); 3 – complex reduction with H_2 (1.2 MPa at increased temperature of 398 K, 8 h); and, 4 – washing with acetone and vacuum drying the Cu-chitosan NC at higher temperature. The second stage was carried out with 0.2 g (12.5×10^{-4} M) of chitosan and 0.12 g (2.4×10^{-4}) of the copper complex (60% of chitosan weight). The calculated ratio was one copper atom per 5 chitosan units. After the reduction stage, the impregnated polymer was washed with acetone to remove the residual unreduced complex and degradation products. Impregnation and reduction were carried out according to the procedure described previously (Said-Galiev et al. 2012).

Preparation of bimetallic blends based on nanoscale $Cu(OH)_2$

Nanoscale $Cu(OH)_2$ was prepared using the procedure described by Dey et al. (2012) with a few modifications. Briefly, 5 g of $CuSO_4 \cdot 5H_2O$ was dissolved in 500 ml of distilled water, followed by the drop-wise addition of NaOH solution (1 M) with constant stirring until the solution attained pH = 12. The procedure took 30 min. The appearance of the deep blue precipitate indicated the formation of $Cu(OH)_2$. Then, the glass with the precipitate was placed in a refrigerator at 269 K overnight. Next day, the precipitate was collected, filtered and washed repeatedly with de-ionized water to remove anions such as sulfate (SO_4^{2-}). The bimetallic blends were prepared by grinding $Cu(OH)_2$ and K_3PO_4 in a particular weight ratio of 1:1 (BB-1) or 3:1 (BB-2) in an agate mortar.

Physicochemical analysis of nanocomposites

X-ray fluorescence analysis (XRF)

Metal content was determined by means of XRF on a "VRA 30" X-ray fluorescent analyzer (Germany) from the line of the M Kα spectrum of X-ray fluorescence (XF). In order to excite XF, an X-ray tube with a Mo anode was used in the 50 kV, 20 μA regime. The powdered chitosan samples containing metal nanoparticles were analyzed as pressed pills. The reference sample for spectrometer calibration was made from a polystyrene and metal salt fine mix, containing n% of a metal, so that in the layer of reference sample with mass 1.23 mg M Kα peak height was created by the metal with mass $1.23 \times 0.n$ = mass of metal (mg). The mass (and thus the concentration) of a metal in the experimental sample were determined by comparing peak height of the composite with that of the reference sample.

Small angles X-ray scattering (SAXS)

SAXS measurements were performed with an "AMUR-K" diffractometer (design of the Institute of Crystallography, Russian Academy of Sciences) at a wavelength $\lambda = 0.1542$ nm with a Kratky-type (infinitely long slit) geometry. Size distributions of heterogeneities

presented in the specimens and those of Cu nanoparticles were computed using the indirect transform program GNOM (Svergun 1992). More detailed information about the experiment and calculations were described previously (Said-Galiev et al. 2011).

X-ray photoelectron spectroscopy (XPS)

X-ray photoelectron spectra were acquired with an Axis Ultra DLD (Kratos, UK) spectrometer using monochromatized Al Kα (1486.6 eV) radiation at an operating power of 150 W of the X-ray tube. Survey and high-resolution spectra of appropriate core levels were recorded at pass energies of 160 and 40 eV and with step sizes of 1 and 0.1 eV, respectively. The sample area of 300 μm × 700 μm contributed to the spectra. The base pressure in the analytical UHV chamber of the spectrometer during measurements did not exceed 10^{-8} Torr. The energy scale of the spectrometer was calibrated to provide the following values for reference samples (i.e, metal surfaces freshly cleaned by ion bombardment): Au $4f_{7/2}$–83.96 eV, Cu $2p_{3/2}$–932.62 eV, Ag $3d_{5/2}$–368.21 eV. Sample charging was corrected by referencing to the C-C/C-H peak deconvoluted in the C 1 s spectrum (284.8 eV). After charge referencing, a Shirley-type background with inelastic losses was subtracted from the high-resolution spectra. The Cu LMM and Zn LMM Auger spectra were corrected using a linear background. The surface chemical composition was calculated using atomic sensitivity factors included in the software of the spectrometer corrected for the transfer function of the instrument.

Transmission electron microscopy (TEM)

Powdered samples were ground in an agate mortar and then placed on a film-coated 200-mesh copper specimen grid. TEM micrographs were performed on Carl Zeiss Leo 912 AB OMEGA electron microscope at accelerating voltage 80 kV.

Screening for antifungal activity

To evaluate the antifungal effects against *R. solani* isolates AG2-Cot9 and AG4-Cot2, three concentrations of chitosan NCs and BBs suspension (30, 60, and 100 μg ml^{-1}) were added to Petri dishes before pouring plates with potato dextrose agar (PDA) according to Tatsadjieu et al. (2009). Each Petri dish was inoculated at the centre with a mycelial disc (10 mm diameter) taken at the margin of an *R. solani* colony grown on PDA at 29 ± 1 °C for 3 days. Positive control (without chitosan NCs and BBs) medium was inoculated by the same method. The growth inhibition percentage was calculated according to the formula of Abd-El-Khair and El-Gamal Nadia (2011):

$$\textit{Growth inhibition}\ (\%) = (\mathrm{C}-\mathrm{P})\Big/\mathrm{C}\ \mathrm{x}\ 100$$

where, C is the diameter of mycelial growth in control plates, and P is the diameter of mycelial growth in treated plates. Five replicates were used per treatment, and the experiment was repeated three times. The chitosan NCs and BBs with the highest levels of inhibition against the pathogens were selected for greenhouse assays.

Production of Rhizoctonia solani inoculum

Two isolates of *R. solani*, AG2-Cot9, and AG4-Cot2 were originally isolated from cotton roots in Egypt. A substrate for growth of isolates was prepared in 500 ml glass bottles, each containing 50 g of sorghum grains and 40 ml of tap water. The bottles with the substrate were autoclaved for 30 min. Isolate inocula, taken from an 1-week-old culture grown on PDA, was aseptically introduced into the bottle and allowed to colonize the sorghum for 3 weeks. The colonized sorghum grains were used to infest soil.

Production of antagonist inoculum

Heavy metal tolerant *Trichoderma longibrachiatum* (hereinafter for simplicity referred to as *Trichoderma)* two strains obtained from Cotton and Fiber Crop Diseases, Plant Pathology Research Institute, ARC, were grown on molasses yeast medium (Papavizas et al. 1984) by liquid fermentation for 14 days, and formulated by mixing 200 ml of fermentor broth with 500 g of autoclaved talc powder. Five grams of carboxymethyl cellulose was added to the powder after air drying and the final dried formulation had a moisture level of 11%. The dry mixture was triturated to a fine powder in a blender.

Effect of seed dressing treatment with bimetallic blends and chitosan nanocomposites combined with Trichoderma longibrachiatum on cotton seedling damping-off

In greenhouse tests, the effects of BBs and chitosan NCs combined with antagonistic *Trichoderma* agents

were evaluated on cotton seedling growth parameters, including preemergence damping-off, postemergence damping-off, survival, plant height, and dry weight. Fifty seeds from cotton cultivar Giza 92 were surface sterilized by gently shaking in 1% NaOCl solution for 3 min and rinsing six times for 5 min in sterile deionized water. Seeds were soaked in 100 μg ml^{-1} BBs and chitosan NCs for 30 min. The *R. solani*-infested sorghum grain was used to infest the autoclaved soil at the rate of 0.1% (*w*/*w*). Infested soil was dispensed into 15 cm diameter clay pots and each pot was planted with 10 seeds. The greenhouse study included the following treatments: *Trichoderma* + BB-1 (T1), *Trichoderma* + BB-2 (T2), 1% acetic acid (T3), *Trichoderma* (T4), BB-1 (T5), BB-2 (T6), Cu-chitosan (T7), *Trichoderma* + Cu-chitosan (T8), Zn-chitosan (T9), *Trichoderma* + Zn-chitosan (T10), high molecular weight chitosan (T11), and infested soil (C). The *Trichoderma* antagonist isolate was evaluated for efficacy in controlling cotton seedlings disease. Seeds of cultivars Giza 92 were infested with the powdered inoculums of each isolate at a rate of 3 g/kg seeds. In the control treatments, sterilized sorghum grains were mixed thoroughly with soil at the previously mentioned rates. Pots were distributed on greenhouse benches in a randomized complete block design. The greenhouse was equipped with a heating system assuring that the minimum temperature in the greenhouse was maintained at 28 °C. There were five replicates (pots) for each treatment. The pots were randomly distributed in the greenhouse. Preemergence damping-off was recorded 15 days after planting. Post-emergence damping-off, survival, plant height (cm), and dry weight (mg/plant) were recorded 45 days after planting. The experiment was repeated once.

Determination of bimetallic blends effects on hyphal morphology

Hyphal morphology of *R. solani* isolates were treated with the highest concentration of BBs (100 μg ml^{-1}). Morphological changes of hyphae resulting from BBs were observed using light microscopy (LaboMed, Los Angeles, USA). This assay enabled the examination of possible morphological changes of the fungus following exposure to BBs to assess antifungal activity. Each assay was repeated at least three times.

Ability of *Rhizoctonia solani* isolates to produce sclerotia in vitro

A 7 mm plug (in diameter) was taken from each of the two *R. solani* isolates and placed in the centre of a 60 mm Petri dish of PDA embedded with the highest concentrations of BBs. Each plate was sealed with parafilm and incubated at 25 ± 2 °C for 18 days. The number of sclerotia was then counted using a transparent grid with subdivisions of 5 mm^2. Each subdivision with 50% or more of its area consisting of sclerotia was recorded and the number of sclerotia calculated (Woodhall et al. 2008). This procedure was replicated three times per isolate.

Fungal genomic DNA binding/degradation and microsatellite primed PCR

Fungal mycelium was produced in 20 ml of liquid medium (24 g l^{-1} of potato dextrose broth [PDB, Difco Laboratories]. Mycelium was harvested by filtration through mesh sieves (40 μm), washed with sterile water, and deposited onto Whatman paper to eliminate excess water. Mycelium was ground to a fine powder in liquid nitrogen using a mortar and pestle. DNA was extracted by the method of Abd-Elsalam et al. (2007). Five microliters of fungal DNA from each *R. solani* AGs was treated with BBs and chitosan NCs (40 μg ml^{-1}) for a period of 2 h at 37 °C. Microsatellite Primed PCR was performed by using T3B primer in a total volume of 25 μL, containing 5 ng of template DNA according to the method of Bahkali et al. (2012). To check the quality of the DNA, seven microliters of the isolated DNA and 3 μl of 10X loading dye were size-fractionated in a 1.5% (*w*/*v*) agarose gel containing 0.05 μg ml^{-1} ethidium bromide. Gel Documentation and Analysis Systems, Uvitec (Cambridge, UK) were used to capture the image.

Statistical analyses

The experimental design was a randomized complete block with five replications in the greenhouse experiment and with five replications in the laboratory test. Data were subjected to analysis of variance (ANOVA). Least Significant Difference (LSD) was used to compare concentration means within genotypes. ANOVA was performed with MSTAT-C statistical package.

Results

Chitosan nanocomposites and nanoscale $Cu(OH)_2$

Due to the structural features, like availability of NH_2- and OH-groups, chitosan can be used as an efficient stabilizer agent for metal nanoparticles. The metal-containing nanoparticles can combine the properties of biopolymer (matrice) and nanosized objects (inclusions) therefore their application when combined can be more effective than separately. In the present study, two chitosan-based nanocomposites with embedded metal nanoparticles were prepared: Zn-chitosan (*via* MVS procedure) and Cu-chitosan (*via* fluid technology – sc CO_2). XRF analysis showed that the metal content (*w*/*w*) in the Cu-chitosan and Zn-chitosan NCs was 5 and 2%, respectively. The metal nanoparticles had a predominantly spherical form and a rather uniform distribution in the chitosan matrice (Fig. 1a, b). In the Cu-chitosan, threadlike-splices consisting of nanoparticles were observed. According to the histogram in Fig. 1c, the size of particles in the Cu-chitosan NC ranged from 1.9 to 5.9 nm with a maximum at about 5 nm. In the case of Zn-chitosan the size of particles ranged from 1.1 to 5.1 nm with a maximum at 3 nm (Fig. 1 c, d). The average particle size in Cu-chitosan and Zn-chitosan composites was 4.1 ± 0.8 nm (mean value ± standard deviation) and 2.0 ± 0.7 nm, respectively.

Calculation of the volume size distribution function - $D_V(R)$- for Cu-chitosan was performed using experimental SAXS curves from the sample on the interval of scattering vectors from 0.4 up to 3.0 nm^{-1}, and the obtained $D_V(R)$ function was compared with the size distribution function of the heterogeneities in the initial chitosan (Fig. 2). The main fraction of the volume size distribution function for the Cu-chitosan NC was a fraction with the sizes of about 2.5–3.0 nm.

For assessing the chemical states of metals in composites, XPS analysis was performed. High-resolution Zn 2p, LMM Auger lines for Zn-chitosan NC are shown

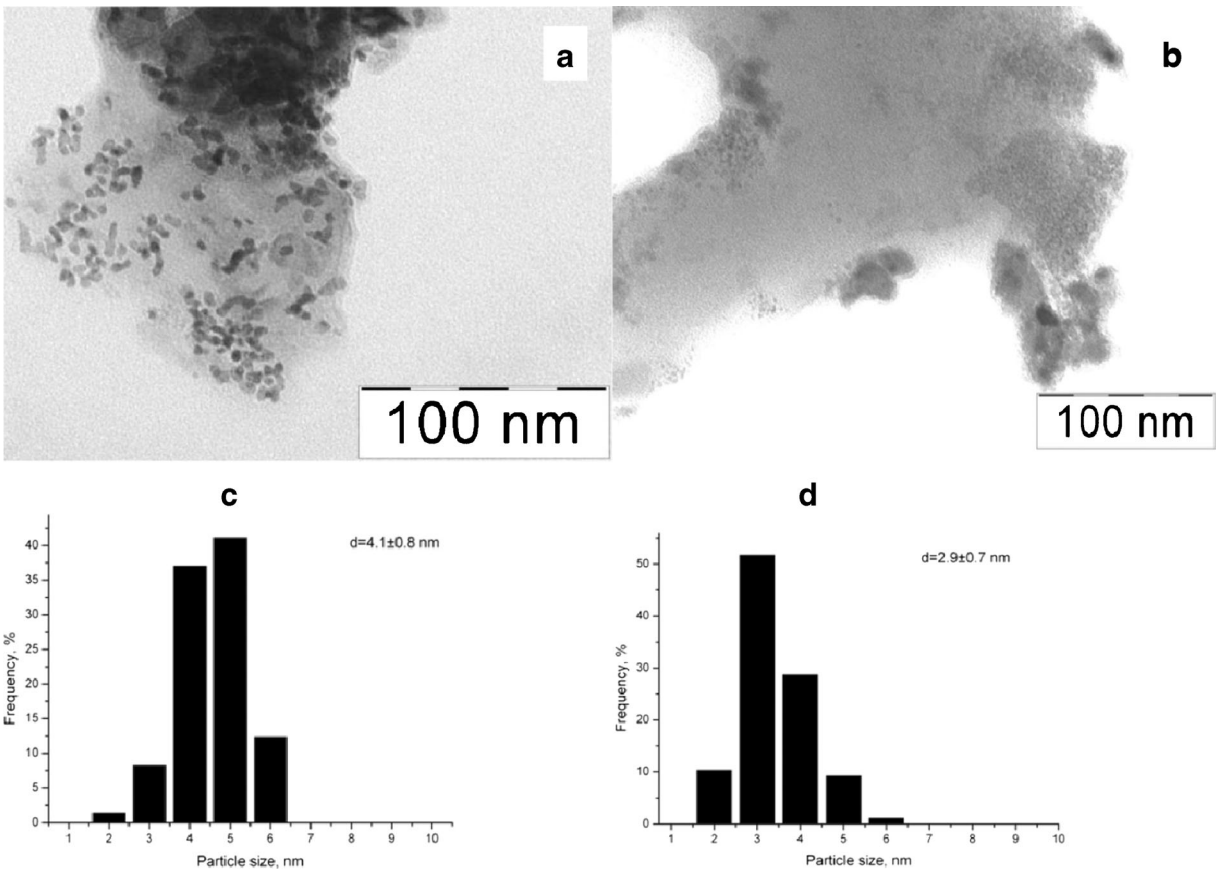

Fig. 1 Transmission electron microscopy micrographs (**a**, **b**) and histograms of the particle size distribution (**c**, **d**) of Cu-chitosan and Zn-chitosan nanocmposites, respectively

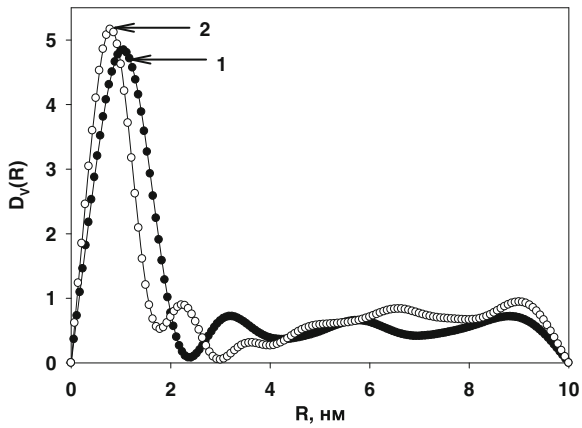

Fig. 2 Volume size distribution functions $D_V(R)$: 1 - Cu-chitosan nanocomposite obtained with the reduction procedure in sc CO_2 medium; 2 – pristine chitosan

in Fig. 3 (left). The binding energies 1021.88 and 1044.92 eV correspond to Zn $2p_{3/2}$ and Zn $2p_{3/2}$ core levels and can be assigned to the ZnO (Naumkin et al. 2012; Barreca et al. 2007a, b; Wöll 2007). It is well known that Zn 2p peaks are not sensitive to the chemical state of zinc atoms (Wöll 2007), while LMM Auger peaks are more sensitive to the chemical environments. The detailed analysis showed that two states with binding energies of 499.63 and 496.58 eV can be resolved in the LMM spectrum. Related Auger parameters 2008.85 and 2011.9 eV can be assigned to ZnO and ZnO_x (Barreca et al. 2007a, b). Relative contents of ZnO and ZnO_x components were 0.52 and 0.48, respectively. Fig. 3 (right) presents the Cu 2p photoelectron spectrum of the Cu-chitosan, which was fitted with three states. The Cu $2p_{3/2}$ peak consisted of three peaks at 932.43, 933.28 and 934.50 eV. The first peak was assigned to the Cu^+ state. The spectrum included satellite peaks at binding energies 943 and 963 eV, which identified the Cu^{2+} state. The Cu $2p_{3/2}$ and Cu $2p_{1/2}$ peaks of the medium state in the Cu $2p_{3/2}$ spectrum had binding energies of 933.27 and 953.14 eV, respectively. The energy of 933.27 eV was 0.6 eV more than that of pure copper foil, and the chemical shift could be assigned to the size effect. Using the data set obtained, Cu 2p spectrum of the Cu-chitosan can be presented as a sum of three states Cu^+, Cu-CN and Cu^{2+} as shown with 23/30/47 intensity ratio, respectively. However, according to the SAXS data the size of copper particles was large enough so that the size effect did not occur. Auger parameter of 1846.50 is rather close to the formation of Cu-CN bonds rather than any possible Cu-O ones (Lindquist and Hemminger 1989). The composition of the composites were $C_{61.8}O_{30.5}N_{7.1}Zn_{0.4}Cl_{0.2}$ (Zn-chitosan) and $C_{55.7}O_{27.8}N_{5.6}Cu_{0.9}F_{9.4}Cl_{0.1}Si_{0.5}$ (Cu-chitosan).

Nanoscale $Cu(OH)_2$ was synthesized by the alkaline hydrolysis of $CuSO_4 \cdot 5H_2O$ using NaOH as a base. According to Dey et al. (2012), at pH 12.0, the rod shaped $Cu(OH)_2$ nanostructures at about 20 nm in diameter and 400–500 nm in length are formed. The BBs were prepared with the grinding of $Cu(OH)_2$ and K_3PO_4 in a particular weight ratio (see Materials and Methods).

Antifungal activity

The effect of three concentrations of BBs and chitosan NCs on mycelial growth of *R. solani* AG-2 is shown in Fig. 4. Intense inhibition of hyphal growth was

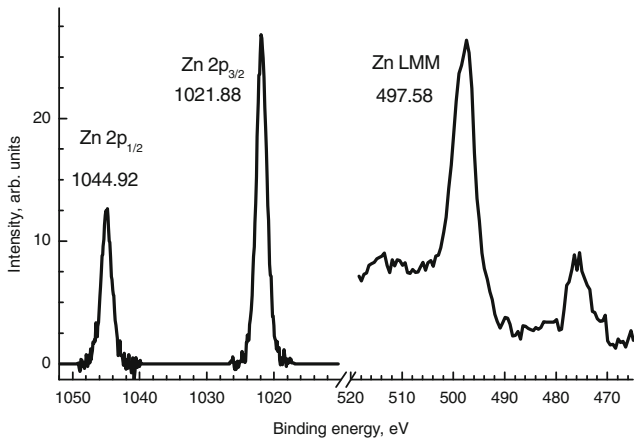

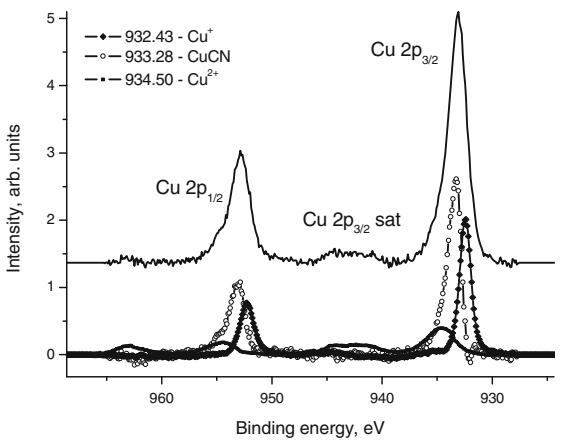

Fig. 3 High-resolution Zn 2p, Zn LMM spectra of Zn-chitosan nanocomposite prepared through deposition procedure of organosol (Zn-toluene) on chitosan (left); high-resolution Cu 2p spectra of Cu-chitosan nanocomposite prepared through the reduction procedure in sc CO_2 medium (right)

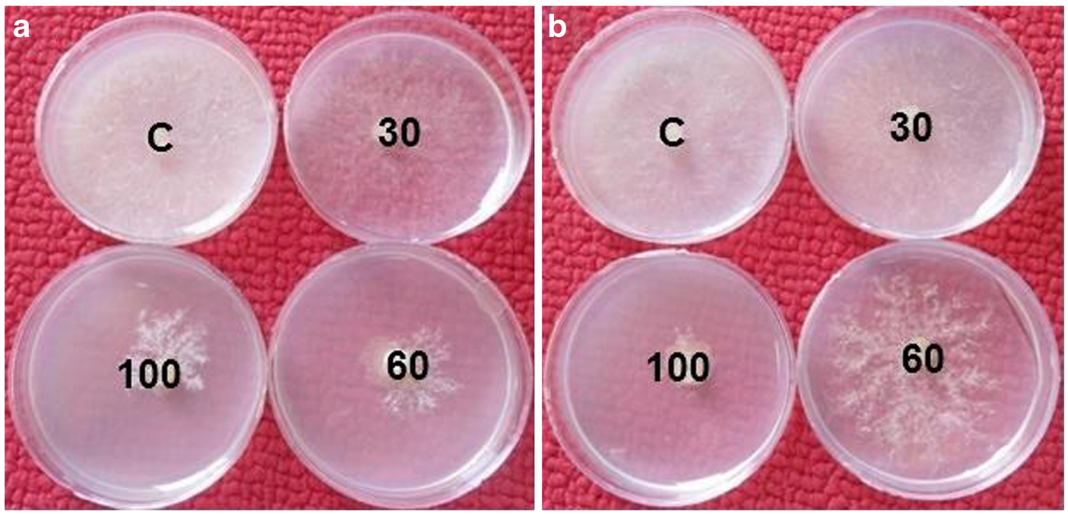

Fig. 4 Effect of different concentrations of bimetallic blends on mycelial growth of *R. solani* (anastomosis group 2) (**a**). Effect of different concentrations of bimetallic blends on mycelial growth of *R. solani* (anastomosis group 4) (**b**)

demonstrated. Changes in hyphal structures were found at the center of the agar medium with irregular objects observed on hyphae (Fig. 4a, b). The highest level of inhibition against *R. solani* AG-2 was found when using the highest concentrations of T5 and T7. The lowest level of inhibition was observed when using the high concentrations of T6 and T9. Since there were significant differences in results between three concentrations of BBs and chitosan NCs, 100 μg ml^{-1} concentration was considered sufficient for antifungal activity (Table 1). The radial growth of *R. solani* was reduced by all concentrations of BBs and chitosan NCs in a dose dependent manner. The highest level of inhibition against *R. solani* AG-4 was observed using the high concentrations of T5 and T7. While the lowest level of inhibition was observed using the high concentrations of T6 and T9. Since there were significant differences in results between three concentrations of BBs and chitosan NCs, 100 μg ml^{-1} concentration was considered sufficient for antifungal activity (Table 1). The antifungal activity of the BBs against *R. solani* appeared to be fungicidal rather than fungistatic, because growth of the fungus transferred from BBs-challenged plates to non-challenged condition was similar to growth of fungus started from untreated plates (Fig. 4).

Control of cotton seedling damping-off

A greenhouse experiment was conducted to determine the effects of BBs and chitosan NCs on cotton seedling disease. Eleven treatments were screened in a greenhouse for control of cotton seedling disease caused by two highly virulent isolates of *R. solani* AGs. The numbers of surviving seedlings cultivated in infested soil amended with *R. solani* were improved by some of the seed treatments with combinations of BBs, chitosan NCs and *Trichoderma*. Other combinations were no better than the individual treatments. When the soil was infested with *R. solani* AG-2, T1 significantly increased the survival while T3 decreased it. T1 and T5 significantly decreased plant height. T1 significantly reduced dry weight of the surviving seedlings (Table 2). Survival and dry weight were not affected by any treatment when soil was infested with *R. solani* AG-4. Plant height was significantly reduced by T3 (Table 3). Surviving seedlings of the cotton cultivar were affected by the type of *R. solani* anastomosis group. There was variation in efficiency of treatments in increasing the number of surviving seedlings, which ranged from 28 to 66% for *R. solani* AG-2 and 40–66% for *R. solani* AG-4 (Table 3). The results of the disease control assays of BBs, chitosan NCs, and *Trichoderma*, and combination of BBs and chitosan NCs plus biological seed treatments for efficacy in the control of pre- and postemergence damping-off in cotton indicated that *Trichoderma* + BB-1 (T1), BB-1 (T5), BB-2 (T6), and Cu-chitosan (T7) gave effective disease control. When cotton seeds were treated with T1 (*Trichoderma longibrachiatum* + $Cu(OH)_2/K_3\ PO_4$) (1:1) under greenhouse conditions, *Trichoderma* mycelium colonized and covered seed coats of grminated seeds and surounding soil 14 days after planting (Fig. 5).

Table 1 Antifungal effect of different concentrations of bimetallic blends and chitosan nanocomposites against the linear growth of *Rhizoctonia solani* (anastomosis group 2 and 4)

Concentrations	Treatments							
	R. solani (AG-2)				*R. solani* (AG-4)			
	[a]T5	T6	T7	T9	T5	T6	T7	T9
30 μg ml^{-1}	[b]0.00	0.00	3.58	3.63	3.30[a]	2.53	3.79	2.53
60 μg ml^{-1}	6.26	3.15	3.88	4.03	5.80	3.35	6.27	4.00
100 μg ml^{-1}	6.80	3.35	4.91	4.63	6.50	4.98	6.80	4.73
Control	0.00	0.00	0.00	0.00	0.00	0.00	0.00	0.00
LSD ($p < 0.05$)	0.49	0.54	0.16	0.62	0.45	0.64	0.53	0.29

[a] T5 = ($Cu(OH)_2$/ K_3PO_4) (1:1), T6 = ($Cu(OH)_2$/K_3PO_4) (1:3), T7 = Cu-chitosan NC, T9 = Zn-chitosan NC. [b] Inhibition zone (cm) and each value is mean of five replications (five plates)

Effect of bimetallic blends on hyphal morphology

The radial growth assays showed inhibition of hyphal growth. The bimetallic blends caused broken mycelia, hyphal lysis or necroses, decrease of the cytoplasm content or cytoplasmic coagulation, irregular shapes of mycelia, and detection of some BBs on hyphal cell walls (Fig. 6). The fungal mycelia from the control sample showed normal, highly branched intact morphology (Fig. 6). The damage on the treated hyphae increased with highest concentration.

Effects of bimetallic blends on sclerotia formation

The effects of tested BBs concentrations on *R. solani* sclerotia formation are presented in Table 4. Non-significant differences ($P > 0{\cdot}05$) were observed in the number of sclerotia produced in vitro between *R. solani* AG-2 and AG-4 treated with BBs. Plates treated with 100 μg ml^{-1} BBs revealed the lowest number of sclerotia compared with control plates. The highest level of inhibition against *R. solani* AG-2 and AG-4 was observed using the highest concentration of T5 (Table 4).

Table 2 Effect of different combinations of bimetallic blends, chitosan nanocomposites, and *Trichoderma longibrachiatum* on incidence of damping-off on cotton seedlings (Cv. Giza 92) grown in soil infested with *Rhizoctonia solani* (anastomosis group 2) under greenhouse conditions

[a]Treatment	Preemergence Damping-off (%)	Postemergence Damping-off (%)	Survival (%)	Plant Height cm	Dry weight mg/plant
T1	22	12	66	13.74	1.038
T2	54	8	38	15.74	1.052
T3	42	40	18	15.88	0.282
T4	48	6	46	16.05	1.184
T5	36	10	54	14.36	1.156
T6	34	12	54	17.31	0.890
T7	36	14	50	15.58	1.174
T8	50	2	48	17.04	1.014
T9	46	6	48	16.64	1.176
T10	52	4	44	20.71	1.052
T11	62	10	28	18.24	0.582
C (infested)	50	8	42	18.10	1.044
LSD ($p < 0.05$)	18.43	16.30	19.66	3.447	0.377

[a] Treatments footnote was described in material and methods. In vitro seed germination of cultivar Giza 92 was 85%

Table 3 Effect of different combinations of bimetallic blends, chitosan nanocomposites, and *Trichoderma longibrachiatum* on incidence of damping-off on cotton seedlings (Cv. Giza 92) grown in soil infested with *Rhizoctonia solani* (anastomosis group 4) under greenhouse conditions.

[a]Treatment	Preemergence Damping-off (%)	Postemergence Damping-off (%)	Survival (%)	Plant Height cm	Dry weight mg/plant
T1	22	12	66	16.86	1.216
T2	42	6	52	19.38	1.322
T3	46	6	48	8.44	1.050
T4	32	8	60	17.89	1.082
T5	30	8	62	17.83	1.010
T6	34	6	60	14.68	1.450
T7	30	6	64	16.52	1.526
T8	58	2	40	18.07	1.126
T9	34	8	58	20.14	1.234
T10	46	10	44	17.96	1.314
T11	44	10	46	13.64	1.172
C (infested)	53	4	44	17.55	1.390
LSD ($p < 0.05$)	19.73	NS	NS	4.882	NS

[a] Treatments footnote was described in material and methods. NS = nonsignificant. In vitro seed germination of cultivar Giza 92 was 85%

Genotoxic effects of bimetallic blends and chitosan nanocomposites

BBs and chitosan NCs, including T5, T6, T7, and T9, were incubated with DNA from the two *R. solani* AGs to evaluate DNA binding activity as a possible molecular basis for their antifungal activities. The genotoxicity exhibited by BBs and chitosan NCs was demonstrated by degradation of *R. solani* DNA at concentrations 40 μg ml^{-1} of the BBs and chitosan NCs. DNA strand scission induced by BBs and chitosan-based NCs led to gradual degradation of linear DNA. Smear bands were appearing towards the lower end of the gel, which were the resultant fragmented DNA (Fig. 7b). Lane 1 and 2 treated with BBs strongly supported that the highest concentration of nanomaterials affected DNA integrity and resulted in significant degradation. There was no effect for T6 treatment on the isolated DNA from *R. solani* AG2. The microsatellite-primed PCR did not amplify genomic DNA treated with concentrations 40 μg ml^{-1} of the bimetallic blends and chitosan nanocomposites for *R. solani* isolates (Lanes 4–8) (Fig. 8b).

Fig. 5 Cotton seedlings from seeds treated with T1 (*Trichoderma longibrachiatum* + $Cu(OH)_2/K_3\ PO_4$) (1:1) after 14 days from planting under greenhouse conditions (30 °C, 85–95% humidity). Yellow arrows mark Cu- tolerant *Trichoderma* mycelium, which colonized and covered seed coats after germination

Discussion

Antifungal activity of BBs and chitosan NCs at concentrations of 30, 60, and 100 μg ml^{-1} was conducted against the fungal pathogen *R. solani*, to reduce and prevent cotton seedlings disease. Previously, Cu–chitosan NPs had exhibited substantial in vitro antifungal activity against *Alternaria alternata*, *Alternaria solani*, *Macrophomina phaseolina* and *R. solani* (Saharan et al. 2013, 2015). Cu-chitosan nanoparticles

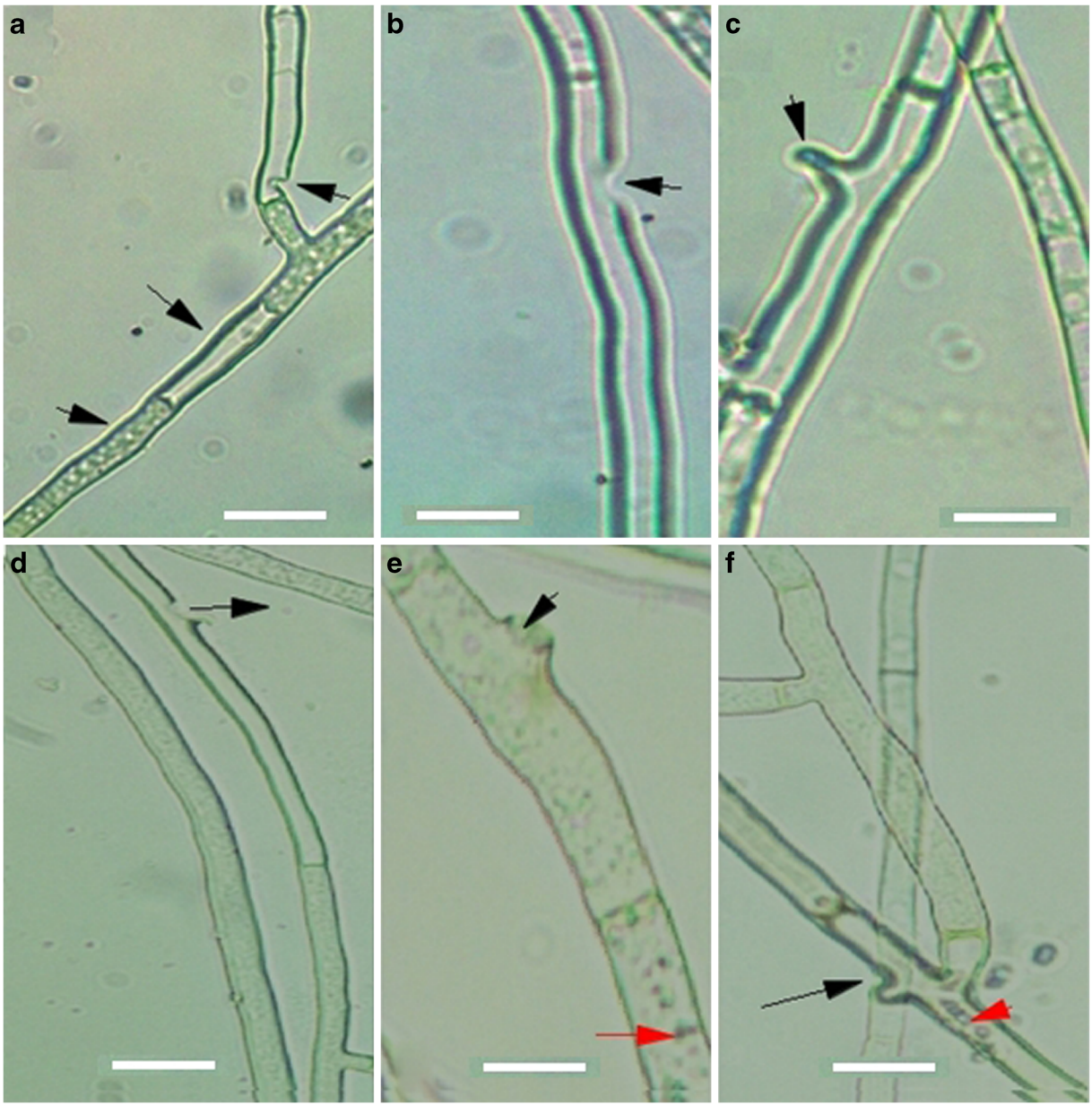

Fig. 6 Light micrograph of the effect of bimetallic blends and chitosan NCs on hyphal morphology of *R. solani* grown on potato dextrose agar, black arrows mark cell wall disruption and necrosis on fungal hyphae. Red arrows mark hyphal fragmentation and cytoplasmic coagulations. Scale bars: **a** = 10 μm, **b–c** = 20 μm, **d** = 10 μm, **e–f** 20 μm

had caused 70.5 and 73.5% inhibition of mycelia growth and 61.5 and 83.0% inhibition of spore germination at 0.12% concentration in *Alternaria solani* and *F. oxysporum*, respectively (Saharan et al. 2015). In the current study, the results of the disease control assays of BBs, chitosan NCs, and *Trichoderma*, and combination of BBs and chitosan NCs plus biological seed treatments for efficacy in the control of pre- and postemergence damping-off in cotton indicated that *Trichoderma* + BB-1 (T1), BB-1 (T5), gave effective disease control. The BBs, *Trichoderma* + BB-1, and Cu-chitosan NC apparently formed an antifungal layer around cotton seeds which protected cotton seedlings from two *R. solani* anastomosis groups. Evaluation of *R. solani* growth inhibition with a biocontrol fungus strain showed synergistic inhibitory effect with

Table 4 Effect of high concentrations of bimetallic blends on sclerotia formation of two *Rhizoctonia solani* anastomosis groups

Concentrations	Anastomosis group			
	R. solani AG-2		*R. solani* AG-4	
	[a]T5	T6	T5	T6
100 μg ml^{-1}	6.000	6.180	4.210	7.997
Control	18.997	19.100	18.997	19.100
LSD ($p < 0.05$)	4.854	4.228	4.854	4.228

[a] T5 = $(Cu(OH)_2/K_3PO_4)$ (1:1), T6 = $(Cu(OH)_2/K_3PO_4)$ (1:3)

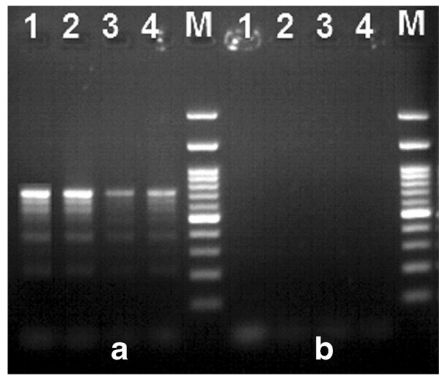

Fig. 8 Microsatellite primed PCR assay of genomic DNA for *R. solani* anastomosis group 4 isolate untreated (**a**) and treated (**b**) with bimetallic blends and chitosan nanocomposites with primer T3B to identify their impact on genotoxicity in *R. solani*

$Cu(OH)_2/K_3PO_4$. The antifungal activities and mode of action of three types of chitosan has been demonstrated against *R. solani* in rice (Liu et al. 2012). The fungal growth decreased with increasing molecular weight for *F. oxysporum* and decreasing degree of acetylation for *A. solani*, but no MW or DA dependences were observed with *A. niger* (Younes et al. 2014). In the current study, the microscopic observation of *R. solani* hyphae exposed to BBs and chitosan NCs showed severe damage resulting in the separation of layers of hyphal wall and collapse of fungal hyphae. The deformation of fungal hyphae treated with Cu NPs and chitosan has been observed in some other fungal pathogens including; *Botrytis cinerea*, *Sclerotinia sclerotiorum, Alternaria alternata* and *Rhizopus stolonifer* (Ouda 2014). The total leakage of cytoplasm by intense activity of chitosan on the fungi *B. cinerea*, *Cylindrocladium floridanum*, *Cylindrocarpon destructans*, *Fusarium acuminatum*, *F. oxysporum,* and *S. sclerotiorum* was also reported by Laflamme et al. (1999), El Hassni et al. (2004), and Ait Barka et al. (2004).

However, much work has to be done regarding the mode of action of chitosan-based nanomaterials against plant pathogens (El Hadrami et al. 2010). It seems that seed treatment with chitosan NCs leads to greater induction of plant defense mechanisms as previously demonstrated by Saharan et al. (2013, 2015). Disruption of protein synthesis and membrane destabilizations is likely primary and secondary modes of antimicrobial action of chitosan (Marquez et al. 2013). Chitosan has been used to control seed-borne fungi of plants as an elicitor rather than a direct toxic agent because it has been reported that chitosan can activate plant defenses in

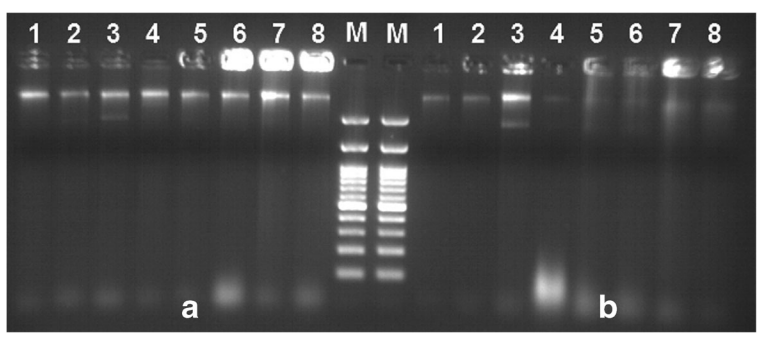

Fig. 7 Agarose gel electrophoretic pattern of the fungal genomic DNA treated with nanocomposites. Lanes 1–4: DNA for untreated *R. solani* AG2 isolates, Lanes 5–8: DNA for untreated *R. solani* AG4 (g DNA, left gel) (**a**). Lane 1: *R. solani* AG2 treated with T5, Lane 2: *R. solani* AG4 treated with T5, Lane 3: *R. solani* AG2 treated with T6, Lane 4: *R. solani* AG4 treated with T6, Lane 5: *R. solani* AG2 treated with T7, Lane 6: *R. solani* AG4 treated with T7, Lane 7: *R. solani* AG2 treated with T9, Lane 8: *R. solani* AG4 treated with T9 (DNA + NCs, right gel) (**b**). DNA treated with BBs and chitosan NCs (40 μg ml^{-1}) showing gradual degradation of the fragmented DNA bands

infected plants (Kaur et al. 2012). Cu-chitosan nanoparticles enhanced enzyme activities involved in plant defense by chitosan participants in the reactive oxygen species (ROS) scavenging system (Saharan et al. 2013, 2015). Nanochitosan upregulates the defense mechanisms which involve enzymes such as phenylalanine ammonium lyase, polyphenol oxidase, tyrosine ammonium lyase and antioxidative enzymes SOD, CAT and POD (superoxide dismutase, catalase and peroxidase) (Ma et al. 2014; Katiyar et al. 2015). The plant microenvironment becomes acidic as a result of fungal infection which leads to the break-up of nanostructure and release of Cu ions (Brunel et al. 2013). The released Cu ions produce reactive hydroxyl radicals to inhibit fungi (Borkow and Gabbay 2005). Cu-chitosan nanonetwork was evident through a higher Cu accumulation in porous areas which supported the ionic and chelating interaction mechanism to suppress enzymes and toxins used by fungal pathogens during pathogenesis (Vahabi et al. 2011). Cu nanoparticles, Cu-chitosan and Zn-chitosan NCs have nearly the same mode of action as Cu-chitosan nanocomposites for instance, the production of ROS, and membrane disruption (Xie et al. 2011; Ingle et al. 2013). Also, zinc is an important micronutrient for plant growth and is absorbed by plants through diffusion and specific transporters in the form of divalent ions. Another important mechanism involves penetration of the chitosan oligomer into the cells of microorganisms which inhibits the growth of cells by preventing the transcription of DNA into mRNA (Hernández-Lauzardo et al. 2011). Cu-chitosan nanocomposites could penetrate cell walls of fungi and bind to DNA or mRNA. Disruption of fungal metabolism and reproduction could ultimately lead to pathogen death.

In the present study, the DNA binding/cleavage efficiency of the BBs and chitosan NCs was investigated after exposure to *R. solani* DNA. Untreated DNA with BBs and chitosan NCs exhibited one major characteristic band of intact genomic DNA while the highest concentration of BBs and NCs affected DNA integrity and resulted in significant degradation. Copper ions released may also interact with DNA molecules and intercalate into nucleic acid strands. Cu nanoparticles degrade DNA in a single oxygen-mediated fashion even in the absence of any external agents like hydrogen peroxide or ascorbate. Low-molecular weight chitosan can penetrate cell walls and interact with cellular DNA of fungi and bacteria which consequently inhibits mRNA transcription and protein synthesis (Xu et al. 2007b). After entering into the cell, Cu NPs may bind with DNA molecules and disturb the helical structure by cross-linking within and between the nucleic acid strands (Ingle et al. 2013). In the current study, BBs and chitosan-based NCs treatment was effective at preventing amplification of PCR products. Oxidative damage can clearly occur with chemical degradation of DNA which leads to PCR amplification failure when insufficient copies of DNA are present in the reaction. Microsatellite primed PCR assay has been successfully used as a potential molecular tool to detect a broad range of DNA changes/alterations caused by nanoparticle-mediated genotoxicity (Moreno-Olivas et al. 2014). Free radicals were known to attack both the base and the sugar moieties of DNA, producing lesions such as single and double-strand breaks, adducts of base and sugar groups, and cross-links to other molecules blocking DNA replication (Sies 1993). In the current study, $Cu(OH)_2/K_3PO_4$ nearly had the same mode of action for Cu-tolerant *Trichoderma* strain such as growth promotion, hyphal distortion and disruption, and genotoxicity.

Concluding remarks

By means of fluid technology (sc CO_2) and metal-vapor synthesis the novel chitosan- based nanocomposites with embedded metal nanoparticles were prepared. Inorganic bimetallic blends (BBs) based on well-known fungicide nanoscale $Cu(OH)_2$ were obtained with the simple route of alkali hydrolysis. The BBs and Cu-chitosan showed the highest antifungal efficacy against both *R. solani* anastomosis groups. The greenhouse evaluation of Cu-chitosan NC and *Trichoderma* combined with BBs showed growth promotion and synergistic inhibitory effect against *R. solani*. This research could lead to the possibility of applying Cu-chitosan NC, BBs and *Trichoderma* as nano biofungicdes at the field level. Light micrographs of *R. solani* mycelia treated with bimetallic nanoparticles showed disruption of hyphal structures. DNA interaction in terms of binding and degradation was also demonstrated. The modes and mechanisms of action of chitosan nanoparticles against microorganisms are not yet fully understood; therefore, further research is needed. It is also

necessary to evaluate the phytotoxic effect involved in the application of nanomaterials in the control of pathogenic fungi.

Acknowledgments The current work was supported by the Science and Technology Development Fund (STDF), Egypt (STDF- RFBR program) [grant no. 13791]. Also, this work was partially funded by Russian Foundation for Basic Research grant (RFBR-15-53-61030).

Compliance with ethical standards

Ethical approval This article does not contain any studies with human participants or animals performed by any of the authors.

Conflict of interest All the Authors declare that they have no conflict of interest.

References

Abd-El-Khair, H., & El-Gamal Nadia, G. (2011). Effects of aqueous extracts of some plant species against *Fusarium solani* and *Rhizoctonia solani* in *Phaseolus vulgaris* plants. *Archives of Phytopathology and Plant Protection, 44*, 1–16.

Abd-Elsalam, K. A., & Alghuthaymi, M. A. (2015). Nanobiofungicides: are they the next-generation of fungicides? *J Nanotech Mater Sci, 2*, 1–3.

Abd-Elsalam, K. A., & Khokhlov, A. R. (2015). Eugenol oil nanoemulsion: antifungal activity against *Fusarium oxysporum* f. sp. *vasinfectum* and phytotoxicity on cottonseeds. *Applied Nanoscience, 5*, 255–265.

Abd-Elsalam, K. A., Asran-Amal, A., & El-Samawaty, A. (2007). Isolation of high quality DNA from cotton and its fungal pathogens. *Journal of Plant Diseases and Protection, 114*, 113–116.

Ait Barka, E., Eullaffroy, P., Clément, C., & Vernet, G. (2004). Chitosan improves development, and protects *Vitis vinifera* L. against *Botrytis cinerea*. *Plant Cell Reports, 22*, 608–614.

Bahkali, A. H., Abd-Elsalam, K. A., Guo, J.-R., Khiyami, M. A., & Verreet, J.-A. (2012). Characterization of Novel Di-, Tri-, and Tetranucleotide microsatellite primers suitable for genotyping various plant pathogenic fungi with special emphasis on Fusaria and *Mycospherella graminicola*. *International Journal of Molecular Sciences, 13*, 2951–2964.

Barreca, D., Comini, E., Ferrucci, A. P., Gasparotto, A., Maccato, C., Maragno, C., Sberveglieri, G., & Tondello, E. (2007a). First example of ZnO-TiO_2 nanocomposites by chemical vapor deposition: structure, morphology, composition, and gas sensing performances. *Chemistry of Materials, 19*, 5642–5649.

Barreca, D., Gasparotto, A., Maccato, C., Maragno, C., & Tondello, E. (2007b). ZnO nanoplatelets obtained by chemical vapor deposition, studied by XPS. *Surface Science Spectra, 14*, 19–26.

Borkow, G., & Gabbay, J. (2005). Copper as a biocidal tool. *Current Medicinal Chemistry, 12*, 2163–2175.

Brunel, F., Gueddari, N. E., & Moerschbacher, B. M. (2013). Complexation of copper (II) with chitosan nanogels: toward control of microbial growth. *Carbohydrate Polymers, 92*, 1348–1356.

Dey, K. K., Kumar, A., Shanker, R., Dhawan, A., Wan, M., Yadav, R. R., & Srivastava, A. K. (2012). Growth morphologies, phase formation, optical & biological responses of nanostructures of CuO and their application as cooling fluid in high energy density devices. *RSC Advances, 2*, 1387–1403.

El Hadrami, A., Adam, L. R., El Hadrami, I., & Daayf, F. (2010). Chitosan in plant protection. *Marine Drugs, 8*, 968–987.

El Hassni, M., El Hadrami, A., Daayf, F., Barka, E. A., & El Hadrami, I. (2004). Chitosan, antifungal product against *Fusarium oxysporum* f. sp. *albedinis* and elicitor of defence reactions in date palm roots. *Phytopathologia Mediterranea, 43*, 195–204.

Fedotov, A. N., Simonov, A. P., Popov, V. K., & Bagratashvili, V. N. (1997). Dielectrometry in supercritical fluids. A new approach to the measurement of solubility and study of dipole moment behavior of polar compounds. *The Journal of Physical Chemistry, 101*, 2929–2932.

Hernández-Lauzardo, A., Velázquez, M., & Guerra-Sánchez, M. (2011). Current status of action mode and effect of chitosan against phytopathogens fungi. *African Journal of Microbiology Research, 5*, 4243–4247.

Ingle, A. P., Duran, N., & Rai, M. (2013). Bioactivity, mechanism of action, and cytotoxicity of copper-based nanoparticles: a review. *Applied Microbiology and Biotechnology, 98*, 1001–1009.

Jans, D., Katia, P., Dian, S., Gerard, B., & Bertrand, G. (2014). Mycotoxin reduction in animal diets. In J. F. Leslie, & A. F. Logrieco (Eds.), *Mycotoxin*.

Joselito, D., & Soytong, K. (2014). Construction and characterization of copolymer nanomaterials loaded with bioactive compounds from *Chaetomium* species. *Journal of Agricultural Technology, 10*, 823–831.

Katiyar, D., Hemantarajan, A., & Sing, B. (2015). Chitosan as a promising natural compound to enhance potential physiological responses in plant: a review. *Indian Journal of Plant Physiology, 20*, 1–9.

Kaur, P., Thakur, R., & Choudhary, A. (2012). An *in vitro* study of the antifungal activity of silver/chitosan nanoformulations against important seed borne pathogens. *International Journal of Scientific & Technology Research, 1*, 83–86.

Kaur, P., Thakur, R., Barnela, M., Chopra, M., Manujaand, A., & Chaudhury, A. (2015). Synthesis, characterization and in vitro evaluation of cytotoxicity and antimicrobial activity of chitosan-metal nanocomposites. *Journal of Chemical Technology and Biotechnology, 90*, 867–873.

Laflamme, P., Benhamou, N., Bussières, G., & Dessureault, M. (1999). Differential effect of chitosan on root rot fungal pathogens in forest nurseries. *Canadian Journal of Botany, 77*, 1460–1468.

Lindquist, J. M., & Hemminger, J. C. (1989). High energy resolution x-ray photoelectron spectroscopy studies of tetracyanoquinodimethane charge transfer complexes with copper, nickel, and lithium. *Chemistry of Materials, 1*, 72–78.

Liu, H., Tian, W. X., Li, B., Wu, G. X., Ibrahim, M., Tao, Z. Y., Wang, Y. L., Xie, G. L., Li, H. Y., & Sun, G. C. (2012). Antifungal effect and mechanism of chitosan against the rice sheath blight pathogen, *Rhizoctonia solani*. *Biotechnology Letters, 34*, 2291–2298.

Ma, L.-J., Li, Y.-Y., Wang, L.-L., Li X.-M., Liu, T., & Bu, N. (2014). Germination and physiological response of wheat (Triticum aestivum) to pre-soaking with oligochitosan. *International Journal of Agriculture and Biology, 16*, 766–770.

Marquez, I. G., Akuaku, J., Cruz, I., Cheetham, J., Golshani, A., & Smith, M. L. (2013). Disruption of protein synthesis as antifungal mode of action by chitosan. *International Journal of Food Micobiology, 164*, 108–112.

Moreno-Olivas, F., Gant, V. U. J., Johnson, K. L., Peralta-Videa, J. R., & Gardea-Torresdey, J. L. (2014). Random amplified polymorphic DNA reveals that TiO_2 nanoparticles are genotoxic to *Cucurbita pepo*. *Journal of Zhejiang University: Science A, 15*, 618–623.

Muzzarelli, R. A. A., Muzzarelli, C., Tarsi, R., Miliani, M., Gabbanelli, F., & Cartolari, M. (2001). Fungistatic activity of modified chitosans against *Saprolegnia parasitica*. *Biomacromolecules, 2*, 165–169.

Naumkin, A. V., Kraut-Vass, A., Gaarenstroom, S. W., & Powell, C. J. (2012). *NIST X-ray photoelectron spectroscopy database, version 4.1*. Gaithersburg: National Institute of Standards and Technology http://srdata.nist.gov/xps/.

Nikitin, L. N., Vasil'kov, A. Y., Banchero, M., Manna, L., Naumkin, A. V., Podshibikhin, V. L., Abramchuk, S. S., Buzin, M. I., Korlyukov, A. A., Khokhlov, A. R. (2011). Composite materials for medical purposes based on polyvinylpyrrolidone modified with ketoprofen and silver nanoparticles. *Russian Journal of Physical Chemistry A, 85*, 1190–1195.

Nikraftar, F., Taheri, P., Rastegar, M. F., & Tarighi, S. (2013). Tomato partial resistance to *Rhizoctonia solani* involves antioxidative defense mechanisms. *Physiological and Molecular Plant Pathology, 81*, 74–83.

Ouda, S. M. (2014). Antifungal activity of silver and copper nanoparticles on two plant pathogens, *Alternaria alternate* and *Botrytis cinerea*. *Research Journal of Microbiology, 9*, 34–42.

Palza, H. (2015). Antimicrobial polymers with metal nanoparticles. *International Journal of Molecular Sciences, 16*, 2099–2116.

Papavizas, G. C., (1984). Strain of *Trichoderma* viride to control Fusarium wilt. U.S. Patent No. 4,489,161, 18 Dec 1984.

Reddy, M. V., Arul, J., Angers, P., & Couture, L. (1999). Chitosan treatment of wheat seeds induces resistance to *Fusarium graminearun* and improves seed quality. *Journal of Agricultural and Food Chemistry, 47*, 1208–1121.

Rubina, M. S., Kamitov, E. E., Zubavichus, Y. V., Peters, G. S., Naumkin, A. V., Suzer, S., & Vasil'kov, A. Y. (2016). Collagen-chitosan scaffold modified with Au and Ag nanoparticles: synthesis and structure. *Applied Surface Science, 366*, 365–371.

Saharan, V., Mehrotra, A., Khatik, R., Rawal, P., Sharma, S. S., & Pal, A. (2013). Synthesis of chitosan based nanoparticles and their *in vitro* evaluation against phytopathogenic fungi. *International Journal of Biological Macromolecules, 62*, 677–683.

Saharan, V., Sharma, G., Yadav, M., Choudhary, M. K., Sharma, S. S., Pal, A., Raliya, R., & Biswas, P. (2015). Synthesis and in vitro antifungal efficacy of Cu–chitosan nanoparticles against pathogenic fungi of tomato. *International Journal of Biological Macromolecules, 75*, 346–353.

Said-Galiev, E. E., Gamzazade, A. I., Grigor'ev, T. E., Khokhlov, A. R., Bakuleva, N. P., Lyutova, I. G., Shtykova, E. V., Dembo, K. A., & Volkov, V. V. (2011). Synthesis of Ag and Cu-chitosan as an metal-polymer nanocomposites in supercritical carbon dioxide medium and study of their structure and antimicrobial activity. *Nanotechnologies in Russia, 6*, 341–352.

Said-Galiev, E. E., Vasil'kov, A. Y., Nikolaev, A. Y., Lisitsyn, A. I., Naumkin, A. V., Volkov, I. O., Abramchuk, S. S., Lependina, O. L., Khokhlov, A. R., Shtykova, E. V., Dembo, K. A., & Erkey, C. (2012). Structure of mono- and bimetallic heterogeneous catalysts based on noble metals obtained by means of fluid technology and metal-vapor synthesis. *Russian Journal of Physical Chemistry A, 86*, 1597–1603.

Sies, H. (1993). Damage to plasmid DNA by singlet oxygen and its protection. *Mutation Research, 299*, 183–191.

Soltani-Nejad, M., Shahidi Bonjar, G. H., Khatami, M., Amini, A., & Aghighi, S. (2016). *In vitro* and *in vivo* antifungal properties of silver nanoparticles against *Rhizoctonia solani*, a common agent of rice sheath blight disease. *IET Nanobiotechnology*. https://doi.org/10.1049/iet-nbt.2015.0121.

Soytong, K., Charoenporn, C., & Kanokmedhakul, S. (2013). Evaluation of microbial elicitors to induce plant immunity for tomato wilt. *African Journal of Microbiology Research, 7*, 1993–2000.

Stoeva, S. I., Smetana, A. B., Sorensen, C. M., & Klabunde, K. J. (2007). Gram-scale synthesis of aqueous gold colloids stabilized by various ligands. *Journal of Colloid and Interface Science, 309*, 94–98.

Svergun, D. I. (1992). Determination of the regnlarization parameter in indirect-transform methods using perceptual criteria. *Journal of Applied Crystallography, 25*, 95–503.

Tatsadjieu, L., Dongmo Jazet, P. M., Ngassoum, M. B., Etoa, F. X., & Mbofung, C. M. F. (2009). Investigations on the essential oil of *Lippia rugosa* from Cameroun for its potential use as antifungal agent against *Aspergillus flavus* Link ex Fries. *Food Control, 20*, 161–166.

Vahabi, K., Mansoori, G. A., & Karimi, S. (2011). Biosynthesis of silver nanoparticles by fungus *Trichoderma reesei*. *Insciences Journal, 1*, 65–79.

Vasil'kov, A. Y., Olenin, A. Y., Titova, E. F., & Sergeev, V. A. (1995). Peculiarities of cobalt nanometer scale particle nucleation on an alumina surface. *Journal of Colloid and Interface Science, 169*, 356–360.

Vasil'kov, A. Y., Naumkin, A. V., Volkov, I. O., Podshibikhin, V. L., Lisichkin, G. V., & Khokhlov, A. R. (2010). Antibacterial and antifungal effect of cotton bandaging material modified with gold nanoparticles. *Surface and Interface Analysis, 42*, 559–563.

Wöll, C. C. (2007). The chemistry and physics of zinc oxide surfaces. *Progress in Surf Science, 82*, 55–120.

Woodhall, J. W., Lees, A. K., Edwards, S. G., & Jenkinson, P. (2008). Infection of potato by *Rhizoctonia solani*: effect of anastomosis group. *Plant Pathology, 57*, 897–905.

Xie, Y., He, Y., Irwin, P. L., Jin, T., & Shi, X. (2011). Antibacterial activity and mode of action of ZnO. *Applied and Environmental Microbiology, 77*, 2325–2331.

Xu, J., Zhao, X., Han, X., & Du, Y. (2007a). Antifungal activity of oligochitosan against *Phytophthora capsici* and other plant pathogenic fungi *in vitro*. *Pesticide Biochemistry and Physiology, 87*, 220–228.

Xu, J., Zhao, X., Wang, X., Zhao, Z., & Du, Y. (2007b). Oligochitosan inhibits *Phytophtora capsici* by penetrating the cell membrane and putative binding to intracellular target. *Pesticide Biochemistry and Physiology, 88*, 167–175.

Xue, J., Luo, Z., Li, P., Ding, Y., Cui, Y., & Wu, Q. (2014). A residue-free green synergistic antifungal nanotechnology for pesticide thiram by ZnO nanoparticles. *Scientific Reports, 4*, 5408. https://doi.org/10.1038/srep05408.

Yoon, M. Y., Cha, B., & Kim, J. C. (2013). Recent trends in studies on botanical fungicides in agriculture. *Plant Pathology Journal, 29*, 1–9.

Younes, I., Sellimi, S., Rinaudo, M., Jellouli, K., & Nasri, M. (2014). Influence of acetylation degree and molecular weight of homogeneous chitosans on antibacterial and antifungal activities. *International Journal of Food Microbiology, 185*, 57–63.